A. Bautista (et al.). *Corrugated stainless steels embedded in carbonated mortars with and without chlorides: 9-Year corrosion results*. Construction and Building Materials 95 (2015) pp. 186–196
DOI: 10.1016/j.conbuildmat.2015.07.099

# Corrugated stainless steels embedded in carbonated mortars with and without chlorides: 9-Year corrosion results

A. Bautista *, S.M. Alvarez, E.C. Paredes, F. Velasco, S. Guzman

*Materials Science and Engineering Department, IAAB, Universidad Carlos III de Madrid, Avda. Universidad n° 30, 28911 Leganés, Madrid, Spain*

## HIGHLIGHTS

- 5 corrugated stainless steels are studied in carbonated mortars.
- Corrosion synergies between carbonation and chlorides are analyzed.
- S32205 duplex shows no corrosion even at high polarizations.
- Partial immersion promotes higher corrosion rates than in non carbonated mortars.

*Keywords:*
Stainless steel
Steel reinforced mortar
Carbonation
EIS
Polarization
Passivity
Pitting corrosion

## ABSTRACT

The corrosion behavior of 5 corrugated stainless steel bars was evaluated in carbonated mortars: UNS S20430, S30400, S31603, S31635 and S32205. The tests were carried out under 3 different exposure con ditions: at high relative humidity (C HRH); partially immersed in 3.5% NaCl (C PI); and with $CaCl_2$ added during mortar mixing and exposed to high relative humidity (C HRHCl). Corrosion potential ($E_{corr}$) mea surements and electrochemical impedance spectroscopy (EIS) were used to monitor the behavior during the first 8 years of exposure. Then, anodic polarization tests were carried out and the exposure was extended for another additional year. Stainless steels do not corrode in carbonated conditions without chlorides, but some grades can suffer localized corrosion if they are submitted to high anodic polariza tions. Low Ni, austenitic S20430 corrugated bars are especially prone to suffer a low intensity corrosive attack in carbonated mortars with chlorides. Moreover, the corrosion rate of S20430 bars can easily increase under moderate anodic polarizations. Duplex S32205 is immune to corrosion in the carbonated mortar with chlorides, even in partial immersion conditions and under high anodic polarizations.

## 1. Introduction

Corrosion of reinforcements often limits the durability of rein forced concrete structures. The corrosion of steel bars is caused by chlorides and/or $CO_2$ from the environment. The carbonation of concrete is associated to the $CO_2$ penetration through the pores. Initially, the concrete is highly alkaline (pH ≈ 12 14) due to the presence of $Ca(OH)_2$ and often of other hydroxides in the pore solu tion. The $CO_2$ that comes from the atmosphere, in presence of water, reacts with the $Ca(OH)_2$. As $Ca(OH)_2$ is consumed, the alka linity of the solution inside the pores decreases. A $CO_3^{2-}/HCO_3^-$ buf fer is often formed, and the pH of the solution decreases to pH values of about 9. At these pHs, carbon steel bars suffer uniform corrosion, because the passive layer that protects the steel at a higher pH is dissolved.

The carbonation process progresses from the surface of the con crete, advancing usually as a quite uniform front. The carbonation rate depends on the diffusion of the gases in the concrete porous network. The penetration rate of the carbonation front is affected by the environmental conditions such as the $CO_2$ concentration [1] and the humidity [1,2], but also on concrete characteristics, such as the size of the aggregates [3], the water/cement ratio [4] or the composition of the cement [5 7].

It has been foreseen that the increasing generation of $CO_2$ emis sions will increase the carbonation rate of concrete structures [8]. A reduction in service lifespan due to carbonation of 15 20 years has been calculated for concrete structures constructed in 2030, in areas with moderate humidity and high temperatures [1]. Hence, carbonation resistant conditions should be especially kept in mind nowadays while designing reinforced structures.

* Corresponding author.
*E-mail address:* mbautist@ing.uc3m.es (A. Bautista).

Substitution of the traditional carbon steel bars by stainless steel bars in the most exposed regions of the concrete structure [9] is an alternative increasingly in use to avoid damages caused by corrosion. Relevant results about the mechanical and structural behavior of corrugated stainless steels in comparison to that of traditional carbon steel reinforcements have been recently published [10]. Moreover, a long term study has analyzed the behavior of different stainless steel corrugated bars in non carbonated mortars with chlorides and their susceptibility to pitting corrosion [11], offering reliable results about the in service behavior of these materials. However, it is also interesting to know in depth the behavior of stainless steel corrugated bars in carbonated concretes. The nature of the passive layers formed on stainless steel at pH 9 is different from that formed at more alkaline pHs [12]. Passive layers of less protective nature are formed in carbonated than in non carbonated solutions [13]. Nevertheless, previous studies in solutions that simulate those contained in the pores of the concrete have proved that no corrosion takes place in stainless steels in carbonated solutions without chlorides [14], suggesting that they can be a good option to assure the durability of structures with a high risk of carbonation.

Moreover, it is interesting to know the response of stainless steels in highly aggressive environments resulting from the simultaneous effect of chlorides and carbonation. This circumstance is not very usual in coastal areas, where low $CO_2$ concentrations and high humidity are typical [4], but it can easily appear in other environments, for example, where the use of de icing salts is common or where contaminated sand is used as aggregate.

The effect of carbonation and chlorides in the corrosion behavior of carbon steel in reinforcements has been studied in solution [15], showing a great dependence not only on the chloride content, but also on the concentration of the $CO_3^{2-}/HCO_3^-$ buffer. Although a common way to express critical chloride threshold to initiate corrosion in reinforced structures is the $[Cl^-]/[OH^-]$ ratio [16], some authors [17,18]have proved that the inhibiting effect of hydroxide ions becomes weaker with decreasing pH. Hence, the carbonation of chloride contaminated structures is an especially dangerous situation if carbon steel reinforcements are used in the most exposed parts. A meaningful fraction of the chlorides that penetrate into the concrete can be chemically and physically bounded to constituents of the cement paste. The degree of chloride binding depends on many factors as the water/cement ratio, the porosity and fineness of the aggregates, the age of the concrete or the cation associated with the chlorides. The key factor for the chloride binding capacity of a concrete is the binder chemical composition (mainly $C_3A$ and $C_4AF$ content) [16,19]. $C_3A$ and $C_4AF$ form chloride bearing salts during their hydration [20]. Reducing the pH in concrete may destabilize the chloroaluminates and thus reduce the percent of bound chlorides [21]. So, carbonation potentially increases the risk that chloride implies for reinforced concrete structures.

Results of stainless steels in carbonated simulated pore solutions with chlorides have also been published. These results show that stainless steels are susceptible to pitting corrosion under these conditions. Their resistance to localized corrosion and the morphology of the attack depend on the composition of the stainless steels [14] and on the processing method of the corrugated bars [22,23]. It has been reported that the thickness of the passive layer formed on stainless steel in carbonated solution decreases as the chloride concentration increases, thus leading to a reduction in the corrosion resistance [24].

Anyway, it has been proved for carbon steels that the critical chloride concentrations that cause corrosion are different when they are obtained from solution tests than when they are obtained using concrete samples [16]. The main reasons for this difference have been previously commented in other article [11]. However, it should be mentioned that there is no significant difference in the critical chloride concentrations obtained in mortar and in concrete tests [16]. Up to now, results of two years have been published about the behavior of a couple of stainless steels in activated fly ash mortar, considering the dual effect of chlorides and carbonation [25], but long term results of corrugated steel in carbonated mortars (with and without chlorides) can offer very interesting, complementary information.

## 2. Experimental

Five different corrugated stainless steels were considered in the study. The bars have been manufactured by Roldán (Acerinox Group) to be used as reinforcements in concrete structures. The diameter of the bars and their mechanical properties can be seen in Table 1. The chemical compositions of the stainless steels (given by the manufacturer) are shown in Table 2. Traditional carbon steel corrugated bars were included in some parts of the study as reference.

The corrugated bars were partly embedded in mortar with a cement/sand/water ratio of 1/3/0.6 (w/w). CEM II/B-L 32.5N was the cement type used to prepare the mortar. The sand was standardized CEN-NORMSAND (according to DIN EN 196-1 standard).

Part of the samples was manufactured with 3% $CaCl_2$ (1.9% Cl), weighed in relation to the cement amount. As a reference, it can be considered that, in European countries and in North America, it has become common practice to limit the tolerable chloride content to around 0.4% of the weight of cement [26].

Cylindrical mortar samples were used (Fig. 1), the thickness of the mortar cover always being 1.5 cm. The length of the bar exposed to the mortar was always 3 cm. The corrugated surfaces of the bars were studied in as-received condition. All cross-sections of the bars embedded in mortar were previously polished to 320# and passivated with $HNO_3$ in the laboratory, in order to reproduce the passivizing process carried out on the corrugated surfaces of the bars in the industry. The surface area exposed to mortar of bars was delimitated using an isolating tape. Ti-activated electrodes [27] where embedded close to the corrugated bars to allow the monitoring of the carbonation front in a subsequent step. Other details about the samples can be found in a previous work [11].

After their manufacturing, the reinforced mortar samples were cured for 30 days at 20 ± 1 °C at high relative humidity (HRH), about 92–93%, and then, the mortar was carbonated. The carbonation process was carried out in a chamber where 10% $CO_2$ enriched air was injected. The temperature in the chamber was 18 ± 1 °C and the relative humidity was between 75% and 80%. The potential of the Ti-electrode was monitored periodically using a saturated calomel electrode (SCE) placed in the outer part of the sample (on the upper surface of the mortar sample). To assure good contact between the mortar and the reference electrode, a small wet pad was used, as it has been plotted in Fig. 1. The carbonation of each sample was determined individually by an abrupt increase in the potential (of about 0.2 V) that corresponds to a change in the pH [28]. In this way, all samples were completely carbonated and errors due to dispersion in the advance of the carbonation front caused by the placement in the chamber were avoided.

After carbonation, the samples were divided into 3 groups and exposed to different aggressive conditions:

- C-HRH: Half of the carbonated samples manufactured without chlorides were exposed at HRH.
- C-PI: The other half of the carbonated samples manufactured without chlorides were partially immersed in 3.5% (w/w) NaCl solution and at HRH. In this case, the level of the solution was kept coinciding with the middle of the exposed length of the bars embedded in the mortar.
- C-HRHCl: The samples manufactured with chlorides were exposed to HRH.

The electrochemical monitoring of the corrosion behavior during the 8-year exposure period was carried out using corrosion potential ($E_{corr}$) and electrochemical impedance spectroscopy (EIS) measurements. To obtain the $E_{corr}$ values, a SCE was used. For the EIS measurements, a three-electrode configuration was used. The surface of corrugated bar exposed to the mortar acted as a working electrode, the reference electrode was a SCE and the counter-electrode was a copper cylinder,

**Table 1**
Mechanical properties and diameter of the five studied stainless steels.

| UNS stainless steel | Diameter (mm) | Tensile strength (MPa) | Yield strength (MPa) | Elongation (%) |
|---|---|---|---|---|
| S20430 | 5 | 918 | 756 | 32 |
| S30400 | 8 | 1035 | 923 | 21 |
| S31603 | 10 | 805 | 521 | 26 |
| S31635 | 12 | 860 | 726 | 22 |
| S32205 | 12 | 1156 | 968 | 12 |

Table 2
Chemical composition of the five studied stainless steels.

| UNS stainless steel | S | C | Ti | Si | Mn | Cr | Ni | Mo | N | Cu | Fe |
|---|---|---|---|---|---|---|---|---|---|---|---|
| S20430 | 0.002 | 0.049 | 0.003 | 0.23 | 8.26 | 16.12 | 1.89 | 0.01 | 0.13 | 2.65 | Bal. |
| S30400 | 0.002 | 0.063 | 0.004 | 0.31 | 1.42 | 18.33 | 8.12 | 0.30 | 0.05 | 0.32 | Bal. |
| S31603 | 0.006 | 0.021 | 0.003 | 0.21 | 1.67 | 17.05 | 10.25 | 2.17 | 0.47 | 0.32 | Bal. |
| S31635 | 0.001 | 0.029 | 0.251 | 0.45 | 1.21 | 16.68 | 11.25 | 2.23 | 0.02 | 0.41 | Bal. |
| S32205 | 0.001 | 0.029 | 0.027 | 0.39 | 1.72 | 22.49 | 4.72 | 3.22 | 0.17 | 0.24 | Bal. |

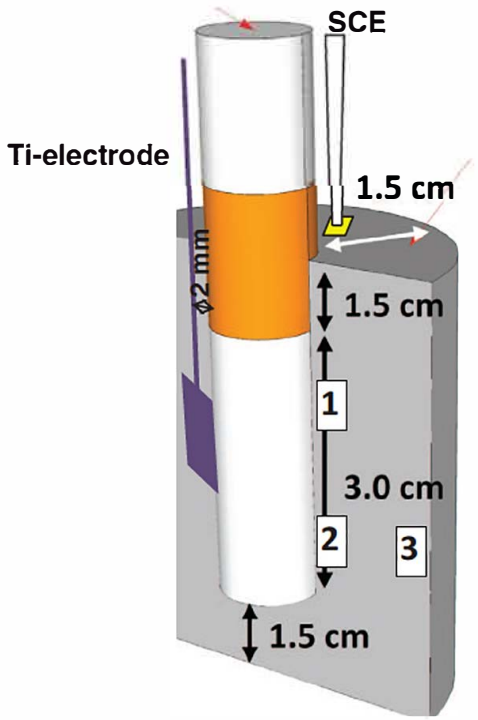


Fig. 1. Scheme of the reinforced mortar specimens manufactured for the study. The regions where the chloride content was measured have been marked as 1–3.

with a diameter slightly higher than that of the mortar sample. To assure a good contact between the mortar and the counter-electrode, a wet pad was used. The EIS spectra were acquired using a perturbation signal of 10 mV rms of amplitude, from $10^3$ to $10^{-3}$ Hz.

After the 8-year exposure period, the reinforced mortar samples were submitted to anodic polarization tests. The tests started from the $E_{corr}$ and potential was increased in steps of 20 mV, with duration of 10 min. When a potential of about 100 mV vs SCE was reached, the length of the steps increased up to 1 h. The increase in the length of the steps is due to higher difficulties of stabilization of the current signal at increasing anodic overpotentials. The polarization steps finished at 900 mV vs. SCE. The current value plotted in the polarization curves used in this work corresponds to the stabilization value of the current after each potential step. More details about this type of tests can be found in [11].

After the polarization tests, the samples were kept for 1 additional year under the exposure conditions to allow the progress or the possible repassivation of the provoked pits. Then, the samples were broken and the morphology and localization of the attack of the bars were studied by scanning electron microscopy (SEM). If this information would have been obtained just after the polarization test, it could have been misleading, as some small provoked pits could have been difficult to detect and the way the pits progress could have been more difficult to evaluate.

The total chloride content of the mortar after the 9-year exposure was measured in three different regions of the samples. The position of the studied regions is marked in Fig. 1. The quantification of the total chloride content was carried out by X-ray fluorescence spectrometry (XRF) [29]. The equipment used was an SPECTRO XEPOS III X-ray Spectrometer with XLabPro 4.5 Software. During each measurement, 4 g of grounded mortar with grain size < 100 μm was analyzed. The samples were excited using a 50 W end-window X-ray tube in a He gas atmosphere and a silicon detector was employed. For screening the analysis results the Turboquant method was used. The given values of Cl concentration are the average of 6 measurements in each region of different samples and they are expressed in relation to the mortar weight.

## 3. Results and discussion

The $E_{corr}$ corresponding to the corrugated bars in carbonated mortar for the 3 different exposure conditions are shown in Figs. 2–4. The criterion suggested by ASTM C876 standard to determine the probability of corrosion for carbon steel reinforcements has also been included in the figures.

In Fig. 2, it can be seen that the $E_{corr}$ of the stainless steel bars exposed to C HRH exhibit values characteristics of the passive state with an occasional value in the border limiting with the region of uncertain corrosion activity. These results suggest that all the stainless steel reinforcements remain passive in carbonated mortar when no chlorides are present. These results are coherent with the predictions drawn from the polarization tests of the bars [14]: no corrosion appears in any of the grades considered in this study during anodic polarizations in pH 9 solutions when no chlorides have been added.

The results of stainless steels are completely different to those of carbon steel in the C HRH condition (Fig. 2). As expected, carbon steel bars show $E_{corr}$ typical of the active corrosion in carbonated mortar without chlorides during the entire exposure.

When the reinforced carbonated mortar samples are partially submerged in NaCl solution (C PI condition), the $E_{corr}$ of the low Ni austenitic S20430 shows a different trend (Fig. 3). For this grade, the $E_{corr}$ suffers a meaningful decrease after 3 years of exposure. In comparison to C HRH, there is now a penetration of chloride ions from the solution to the reinforcements with time. Moreover, cells that favor the corrosion process can appear between the submerged and the non submerged part of the sample. Aeration cells are formed due to the different $O_2$ access (much more limited in the submerged region), thus favoring the location of the anodes on the submerged surface of the bar. Other concentration cells could also appear (i.e.: Cl ), fostering the corrosion in the submerged part of the bar.

In non carbonated conditions [11], the partially immersed exposure has provoked a low intensity corrosive attack after 7 years of exposure on low Ni austenitic S20430. When the mortar is carbonated (Fig. 3), the results of $E_{corr}$ suggest an even higher aggressivity.

In Fig. 3, it can also be seen that the traditional austenitic S30400 has $E_{corr}$ in the uncertain activity region during several years, though the $E_{corr}$ recovers values characteristic of passivity at the end of the exposure. On the other hand, considering the $E_{corr}$ results, the presence of Mo in stainless steels (as S31603 or the duplex microstructure of S32205) seems to completely guarantee the stability of the passivity in C PI conditions.

The limited corrosion resistance of S20430 in C PI is coherent with the results of the polarization tests previously carried out in carbonated solutions with chlorides [14] where the limited length of the passive region was shown. The $E_{corr}$ behavior during the long term C PI exposure of the other austenitic stainless steels and of the duplex stainless steel is also coherent with the results of polarization tests in carbonated solutions with chlorides [14,30] where longer passive regions were detected. Moreover, the different protective nature of their passive films formed in carbonated conditions on the studied stainless steels grades and

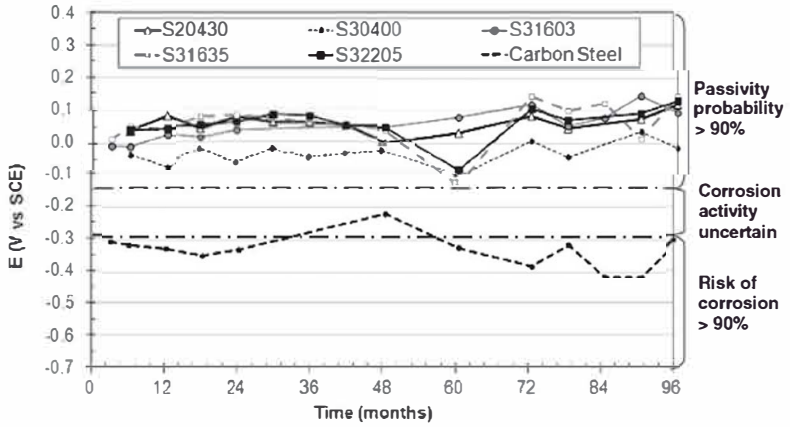


Fig. 2. $E_{corr}$ of the reinforced mortar samples exposed in C-HRH condition.

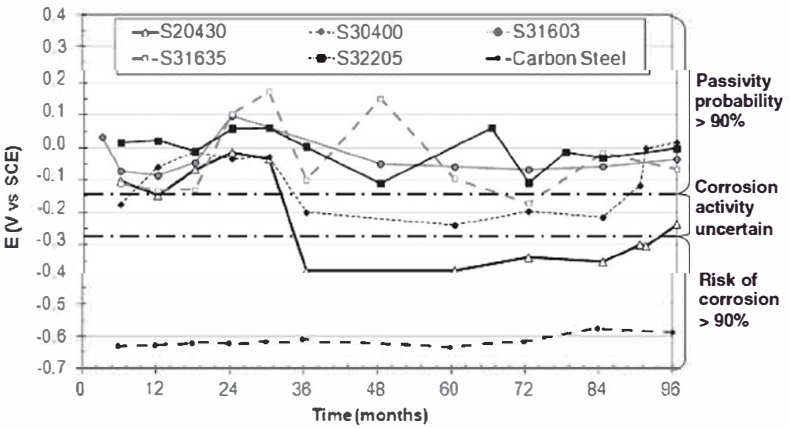


Fig. 3. $E_{corr}$ of the reinforced mortar samples exposed in C-PI condition.

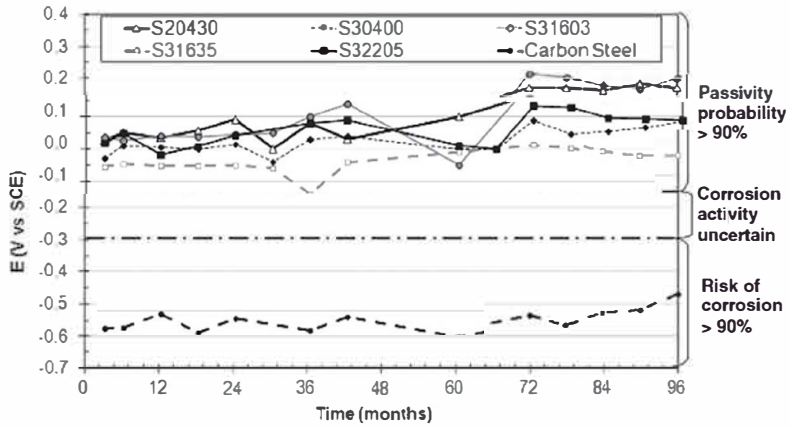


Fig. 4. $E_{corr}$ of the reinforced mortar samples exposed in C-HRHCl condition.

analyzed by X ray photoelectron spectroscopy (XPS) can also justify the $E_{corr}$ trends observed in Fig. 3 (i.e. chromium rich oxides for S32205 and iron rich oxides also comprising also poorly protective Mn oxide for S20430) [13].

On the other hand, the $E_{corr}$ of the carbon steel bars in C PI are always typical of an active corrosion (Fig. 3). But it must be pointed out that the $E_{corr}$ values are, in this case, much more negative than those measured for the carbon steel in C HRH (Fig. 2). The foreseen decrease in the mortar electrical resistance due to the presence of chlorides in the C PI is not enough to explain this difference. The $E_{corr}$ measured in the C PI are even lower than those measured for carbon steel in non carbonated partially immersed samples (PI in [11]). The low $E_{corr}$ measured in C PI suggest an increased corrosion activity of the carbon steel since the first months of exposure, in comparison to the values measured in C HRH.

When the chlorides are added during the manufacturing of the samples (C HRHCl condition), the stainless steel reinforcements show $E_{corr}$ values (Fig. 4) similar to those observed for the C HRH

condition (Fig. 2). It is worth remembering that an identical amount of chlorides added during manufacturing has previously been proved to be unable to cause pitting in stainless steels when the mortar was not carbonated [11]. These results demonstrate that the foreseen decrease on the pitting resistance due to carbon ation is not enough, for this chloride concentration, to break the passivity of the stainless steel reinforcements.

The $E_{corr}$ of the carbon steel samples in C HRHCl condition (Fig. 4) are typical of the active state, with values lower than those found for the same material in absence of chlorides (C HRH, Fig. 2), but somewhat higher than those detected in the C PI condition (Fig. 3).

The total chloride content of the samples (in relation to the mortar weight) has been calculated after 9 years of exposure using XRF. Material from three different regions of the samples has been analyzed: Region 1 mortar close to the upper part of the bar (in C PI condition, from the aerated region); Region 2 mortar close to the lower part of the bar (in C PI condition, from the submerged region); Region 3 mortar from the outer surface of the samples (in C PI condition, from the submerged region). The localization of these regions in the sample is plotted in Fig. 1.

Obviously, no chlorides are detected in any region of the sam ples after the C HRH exposure. Results of chloride concentrations after C PI and C HRHCl are plotted in Fig. 5. Bearing in mind the error bars (associated with the variability of the Cl amount in equivalent regions of different samples), it can be assumed that, for a given exposure condition, the chloride contents are quite sim ilar all over the mortar samples after 9 years. Though the chlorides penetrate into the mortar from the NaCl solution and Cl concen tration gradients must have existed at the beginning of the expo sure, the duration of the tests has been long enough to homogenize the Cl concentration by diffusion [31]. The influence of possible Cl concentration cells formed on the surface of the bars in C PI can be disregarded for long term exposures of this kind of samples.

The average Cl concentration of the mortars in the C HRHCl could be considered slightly higher than that of the mortars in C PI. However, bearing in mind the overlapping of the error bars, the relevance of the differences found for the average values is questionable. Moreover, chlorides added during the manufacturing of the mortar (C HRHCl) probably have a higher bonded fraction of these ions. It is well known that, during curing, some chlorides become physically and chemically bonded to the hydration prod ucts of the cement. When chlorides are bound, they represent a lower risk for the pitting corrosion, though they can play a certain role in pitting initiation [32], as a large part of the bound chlorides are released as soon as the pH drops to values below 12 [21]. Moreover, calcium chloride (added to C HRHCl) leads to more bonded chlorides than sodium chloride (added to C PI) [16,33]. Thus, it could be assumed that it is possible that, in spite of the val ues shown in Fig. 5, Cl can be present in a more corrosive way in C PI than in C HRHCl. The well known importance of $O_2$ concen tration cells is confirmed as a key to explain the aggressivity of the C PI exposure.

Chloride concentrations determined for C HRHCl (Fig. 5) are logically similar to those measured for non carbonated mortars with added chloride [11], but a lower fraction of bounded chlorides is expected in this case, due to the carbonation of the mortar.

However, the amount of chlorides detected in non carbonated samples after 9 years of partial immersion in 3.5% NaCl [11] is (about 5 times) higher than when the samples are carbonated. These results confirm that carbonates precipitate inside the pores due to $Ca(OH)_2$ reaction with $CO_2$, reducing the permeability of the mortar [34], and informs that this phenomenon is able to limit the amount of chlorides that penetrate. Anyway, the fact that the S20430 decreases its $E_{corr}$ to the region of corrosion before in the C PI than in partial immersion without carbonation [11] stresses the high importance that a decrease on the pH of the concrete might have on the durability of some stainless steel reinforcements where there are chlorides in the medium.

As $E_{corr}$ values offer only probabilistic information, and that information has been extensively checked for carbon steel rein forcements but not for stainless steels, it has been considered nec essary to match these data with those obtained from EIS studies. In Fig. 6, two examples of the EIS spectra obtained for the stainless steel reinforced carbonated samples can be seen. In Fig. 6(a), the spectrum of a sample whose $E_{corr}$ is in the passive region can be seen, while in Fig. 6(b) the spectrum of a sample whose $E_{corr}$ is in the active region appears. The fitted data obtained from the simu lation of both examples are also included in the figure. The equiv alent circuit previously used to simulate the behavior of stainless steel reinforced non carbonated mortars [11] has also proved to

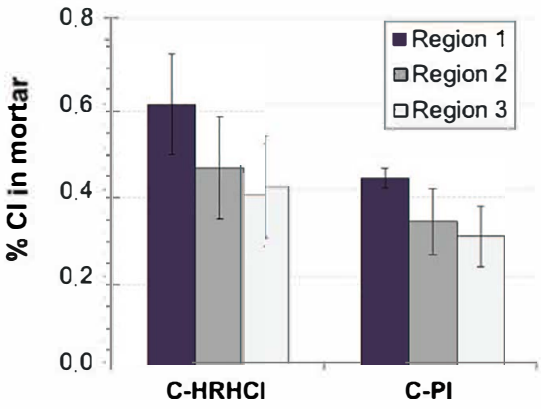


Fig. 5. Chloride concentration (% by wt. to mortar) after 9 years of exposure.

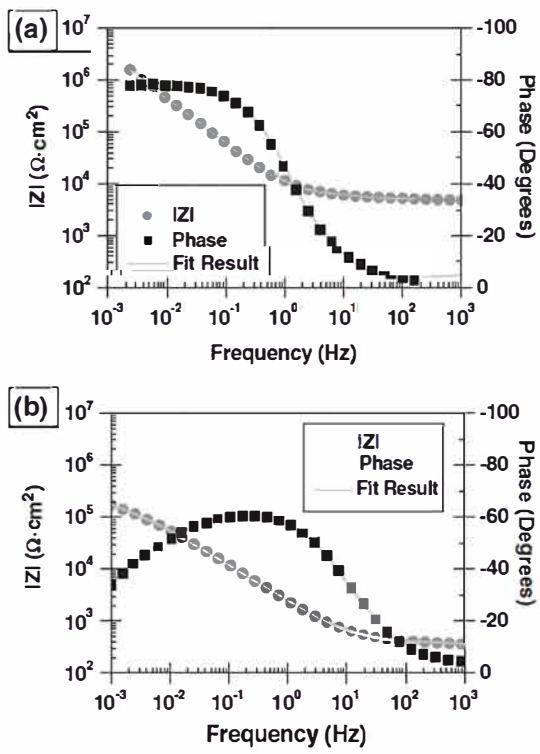


Fig. 6. Experimental data and fitted curve of the EIS spectra corresponding to stainless steel bars in carbonated mortars after 60 months of exposure: (a) S31603 in C-HRH; (b) S20430 in C-PI.

be adequate to simulate the EIS spectra of the carbonated samples. The equivalent circuit consists in a resistance that reproduces the resistive behavior of the mortar ($R_m$) in series with two time constants in cascade [11].

The medium frequencies time constant is formed by a resistance ($R_{pl}$) and a constant phase element ($CPE_{pl}$) that has been identified with the electrochemical behavior of the passive layer. As this time constant also appears when EIS studies of stainless steels in the simulated pore solutions are carried out [13,35,36] and no cementitious film precipitates on the surface of the rebars during these tests, this behavior should be identified with other phenomena taking place on the surface of the bars. A redox process related to the oxides in the passive film has been sometimes suggested [37,38] but also this time constant has been related to resistance of the ionic paths through the passive film and the capacitance associated to dielectrical behavior of this layer [36].

The low frequency time constant is constituted by the charge transfer resistant ($R_t$) in parallel with the constant phase element corresponding to the capacitive behavior of the double layer ($CPE_{dl}$). The identification of this low frequency time constant with the charge transfer step is usual in the published literature about stainless steels in alkaline media [11,13,35,37,39].

The $R_m$ is an interesting parameter, as it often determines the corrosion rate of carbon steel reinforced concrete structures. Obtained $R_m$ values depend on the testing conditions, but they are independent from the nature of the reinforcement (if no cracking of the cover takes place, as occurs with stainless steel reinforcements). In Fig. 7, the evolution with time of average $R_m$ values for all the tested samples are plotted for each exposure condition. The C HRH condition causes the highest $R_m$ values. The presence of Cl in solution inside the pores of the samples in C HRHCl conditions explain the decrease of the $R_m$ values in comparison with those determined for C HRH. The partial immersion in NaCl assures the saturation of the pores with electrolyte, at least in the lower part of the samples. These facts explain the lower $R_m$ values determined for C PI. Anyway, a lower level of bounded chlorides in C PI than in C HRHCl and differences in the curing process can also contribute to this difference.

If the $R_m$ values in Fig. 7 are compared to those determined for the same parameter in non carbonated mortars (Fig. 7 in [11]), the initial increase in the $R_m$ observed for the non carbonated mortars cannot be observed in carbonated ones. This fact is due to the higher curing level of the carbonated mortars when they are exposed to the testing environments (the carbonation process lasted a few weeks). $R_m$ in C HRH is higher than $R_m$ determined for non carbonated mortar exposed in the same condition (HRH in [11]) due to the precipitation of carbonates inside the pores. $R_m$ values determined for C PI are lower than $R_m$ determined for

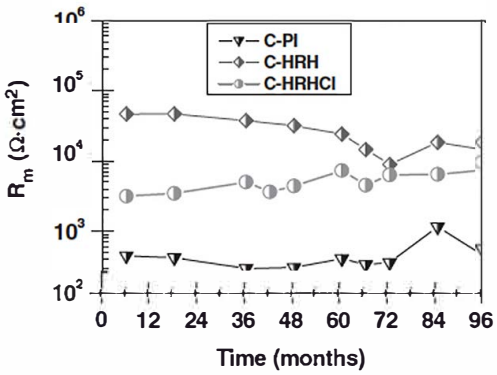


Fig. 7. Average $R_m$ values obtained from the EIS spectra for the stainless steel reinforced mortar samples in the different exposure conditions.

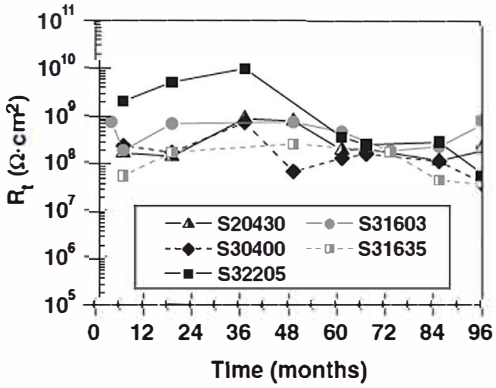


Fig. 8. $R_t$ values obtained from the EIS spectra of the stainless steels in C-HRH condition.

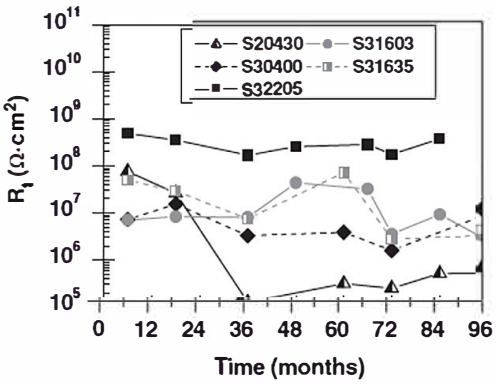


Fig. 9. $R_t$ values obtained from the EIS spectra of the stainless steels in C-PI condition.

non carbonated mortars under partial immersion [10], that is to say, carbonation decreases the mortar resistance when the samples are partially immersed in NaCl. However, the chloride amount penetrated from the solution to the mortar surface is higher in non carbonated conditions (compare results in Fig. 5 with those on Fig. 3 in [11]). The fraction of bounded chlorides in carbonated mortars should be lower than in non carbonated mortars to explain this fact. The influence of carbonation in the chloride binding ability of the mortars has been also suggested by results obtained by other authors [40]. Friedel's salt is the main solid phase formed from the reaction between chlorides and a hydrated cement paste [20]. In presence of $CO_2$(g), the decrease of the pH causes Friedel's salt instability and bounded Cl ions are liberated to the pore solution [20].

The $R_t$ values from the EIS spectra are plotted in Figs. 8–10 for the different exposure conditions. In Fig. 8, it can be seen that for C HRH, $R_t$ exhibit high values, the order of magnitude of which is similar to that of passive stainless steels in non carbonated mortars (Fig. 10 in [11]). These values confirm the passive state suggested by the $E_{corr}$ (Fig. 2).

In Fig. 9, it can be seen that the $R_t$ of the S20430 in C PI decreases nearly two orders of magnitude when its $E_{corr}$ passes from the passivity region to the corrosion region (Fig. 3). The pitting of low Ni stainless steel in carbonated alkali activated fly ash mortars with chlorides has been reported by other authors [25], confirming the limitations that this grade can have for its use in extremely aggressive conditions.

S30400 stainless steel, whose $E_{corr}$ remained for long periods in the region of uncertain corrosion activity in C PI (Fig. 3), exhibits $R_t$

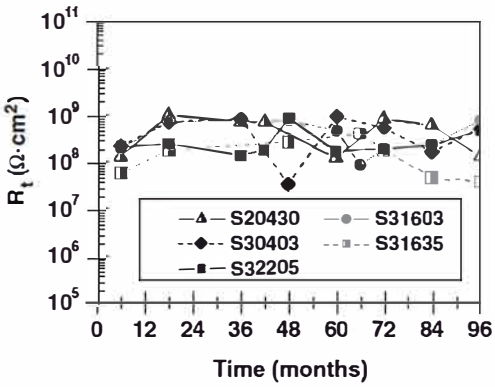


Fig. 10. $R_t$ values obtained from the EIS spectra of the stainless steels in C-HRHCl condition.

values (Fig. 9) slightly lower than those usual for passive stainless steel reinforcements. In the period when the $E_{corr}$ was in the region of uncertain activity, the calculated $R_t$ are below $10^7\ \Omega\ cm^2$. Identifying $R_t$ with the polarization resistance in the Stem Geary equation implies $i_{corr}$ of the order of $nA$, that is to say, the S30400 can be considered at passive state, in spite of the ambiguous value of its $E_{corr}$ if it is interpreted following the criterion defined in ASTM C876 for carbon steel. Anyway, the behavior of S30400 in C PI seems to be coherent with the results of the polarization tests, where this grade exhibits a pitting resistance in chloride containing carbonated solutions lower than those of more alloyed/more expensive grades as S31603 or S32205 [13].

For the other stainless steels, the EIS simulation of the spectra obtained from samples in C PI gives $R_t$ values (Fig. 9) typical of the passive state, as their $E_{corr}$ have suggested (Fig. 3). The S32205 stands out because of its high $R_t$ value (admitting the uncertainty that implies the extrapolation of the experimental data to very low frequencies needed to obtain such high resistance values).

Comparing the results obtained in our laboratory for the $R_t$ corresponding to S20430 in C PI with those of the same material in non carbonated mortar in partial immersion in 3.5% NaCl [11], it can be deduced that the low intensity attack the S20430 tend to suffer in partial immersion exposures starts before when the mortar is carbonated. This occurs because much lower Cl concentration is needed to break the passivity at lower pHs. Moreover, when the attack starts, it seems to progress at higher rates in carbonated mortars.

In C HRHCl conditions (Fig. 10), the $R_t$ values are high, confirming the information about the passive state that can be deduced from the $E_{corr}$ (Fig. 4). If values in Fig. 10 are compared with those in Fig. 8, no meaningful differences in $R_t$ can be found due to addition of chlorides during mixing.

The values corresponding to other parameters obtained from the simulation of the EIS spectra can be seen in Tables 3 5. $C_{pl}$ and $n_{pl}$ are, respectively, the capacitance and the parameter that quantifies the deviation of the ideal behavior for $CPE_{pl}$, being $CPE_{pl} = 1/[C_{pl}(j\omega)^n]$. $C_{dl}$ and $n_{dl}$ are the same parameters corresponding to $CPE_{dl}$. The data in the tables confirm that the corrosion rate is controlled by a low frequency time constant ($R_t$ is orders of magnitude higher than $R_{pl}$), so the estimations of $i_{corr}$ made before using the Stern Geary equation are correct.

In Tables 3 5, $C_{dl}$ is in the range of values usually assumed for this parameter. It is not easy to see any meaningful evolution in the values of the different parameters with time in any condition. However, it is clear that $R_{pl}$ shows lower values in C PI conditions, intermediate values in C HRHCl and higher values in C HRH. That is to say, the presence of chlorides decreases the resistance of the passive layer, and this decrease is more marked when the samples are partially immersed. Moreover, carbonated samples with

**Table 3**
EIS parameters obtained for samples exposed in C-HRH, different from those plotted in Figs. 7 and 8.

| Steel Type | Exposition time (months) | $C_{pl}$ ($\mu F\ cm^2\ s^{n-1}$) | $n_{pl}$ | $R_{pl}$ ($k\Omega\ cm^2$) | $C_{dl}$ ($\mu F\ cm^2\ s^{n-1}$) | $n_{dl}$ |
|---|---|---|---|---|---|---|
| S20430 | 6 | 6.0 | 0.76 | 19 | 8.2 | 0.74 |
| | 18 | 4.5 | 0.76 | 11 | 9.4 | 0.74 |
| | 36 | 5.0 | 0.76 | 8.1 | 10 | 0.74 |
| | 60 | 4.3 | 0.77 | 11 | 10 | 0.75 |
| | 66 | 8.0 | 0.77 | 9.5 | 8.4 | 0.74 |
| | 96 | 11 | 0.76 | 19 | 11 | 0.75 |
| S30400 | 6 | 8.0 | 0.83 | 40 | 8.9 | 0.81 |
| | 18 | 8.5 | 0.84 | 30 | 9.4 | 0.82 |
| | 36 | 10 | 0.86 | 25 | 9.6 | 0.83 |
| | 60 | 6.6 | 0.85 | 12 | 14 | 0.85 |
| | 96 | 11 | 0.85 | 3.8 | 26 | 0.85 |
| S31603 | 6 | 10 | 0.98 | 9.4 | 18 | 0.86 |
| | 18 | 13 | 0.91 | 13 | 13 | 0.89 |
| | 48 | 14 | 0.90 | 22 | 9.9 | 0.89 |
| | 60 | 15 | 0.90 | 20 | 8.2 | 0.89 |
| | 72 | 12 | 0.90 | 6.6 | 12 | 0.89 |
| | 96 | 13 | 0.89 | 10 | 9.4 | 0.88 |
| S31635 | 6 | 4.9 | 0.86 | 5.8 | 31 | 0.87 |
| | 18 | 18 | 0.89 | 26 | 16 | 0.87 |
| | 48 | 16 | 0.88 | 19 | 16 | 0.86 |
| | 60 | 19 | 0.85 | 9.5 | 30 | 0.82 |
| | 72 | 7.8 | 0.79 | 8.9 | 22 | 0.86 |
| | 96 | 16. | 0.84 | 9.2 | 25 | 0.86 |
| S32205 | 6 | 5.6 | 0.80 | 40 | 11 | 0.78 |
| | 18 | 4.8 | 0.79 | 30 | 11 | 0.77 |
| | 36 | 6.9 | 0.79 | 23 | 9.9 | 0.77 |
| | 60 | 12 | 0.58 | 4.6 | 49 | 0.70 |
| | 66 | 9.3 | 0.78 | 28 | 8.0 | 0.75 |
| | 96 | 7.0 | 0.75 | 12 | 11 | 0.73 |

**Table 4**
EIS parameters obtained for samples exposed in C-PI, different from those plotted in Figs. 7 and 9.

| Steel type | Exposition time (months) | $C_{pl}$ (μF cm$^2$ s$^{n\ 1}$) | $n_{pl}$ | $R_{pl}$ (kΩ cm$^2$) | $C_{dl}$ (μF cm$^2$ s$^{n\ 1}$) | $n_{dl}$ |
|---|---|---|---|---|---|---|
| S20430 | 6 | 19 | 0.89 | 1.1 | 18 | 0.88 |
| | 18 | 13 | 0.85 | 0.7 | 18 | 0.84 |
| | 36 | 53 | 0.79 | 0.3 | 66 | 0.77 |
| | 60 | 80 | 0.64 | 0.2 | 32 | 0.87 |
| | 72 | 70 | 0.68 | 0.5 | 19 | 0.89 |
| | 96 | 82 | 0.70 | 0.6 | 22 | 0.93 |
| S30400 | 6 | 28 | 0.83 | 0.6 | 33 | 0.83 |
| | 18 | 17 | 0.87 | 0.3 | 24 | 0.87 |
| | 36 | 38 | 0.83 | 0.2 | 37 | 0.81 |
| | 60 | 30 | 0.85 | 0.2 | 43 | 0.84 |
| | 72 | 34 | 0.83 | 0.5 | 33 | 0.81 |
| | 96 | 28 | 0.87 | 0.1 | 26 | 0.87 |
| S31603 | 6 | 26 | 0.89 | 0.3 | 27 | 0.87 |
| | 18 | 34 | 0.92 | 0.6 | 14 | 0.83 |
| | 36 | 37 | 0.79 | 0.1 | 35 | 0.78 |
| | 72 | 31 | 0.82 | 0.2 | 42 | 0.81 |
| | 96 | 58 | 0.83 | 6.7 | 16 | 0.98 |
| S31635 | 6 | 29 | 0.89 | 4.0 | 13 | 0.89 |
| | 18 | 22 | 0.87 | 1.8 | 14 | 0.86 |
| | 36 | 37 | 0.83 | 2.5 | 12 | 0.82 |
| | 60 | 19 | 0.84 | 1.1 | 14 | 0.83 |
| | 72 | 22 | 0.80 | 0.4 | 18 | 0.78 |
| | 96 | 11 | 0.98 | 0.2 | 47 | 0.78 |
| S32205 | 6 | 59 | 0.83 | 3.7 | 53 | 0.87 |
| | 18 | 46 | 0.81 | 1.1 | 54 | 0.78 |
| | 36 | 53 | 0.82 | 0.9 | 55 | 0.84 |
| | 66 | 75 | 0.82 | 2.2 | 40 | 0.83 |
| | 72 | 66 | 0.79 | 1.8 | 51 | 0.77 |
| | 84 | 31 | 0.77 | 3.0 | 62 | 0.80 |

**Table 5**
EIS parameters obtained for samples exposed in C-HRHCl, different from those plotted in Figs. 7 and 10.

| Steel type | Exposition time (months) | $C_{pl}$ (μF cm$^2$ s$^{n\ 1}$) | $n_{pl}$ | $R_{pl}$ (kΩ cm$^2$) | $C_{dl}$ (μF cm$^2$ s$^{n\ 1}$) | $n_{dl}$ |
|---|---|---|---|---|---|---|
| S20430 | 6 | 14 | 0.83 | 3.0 | 22 | 0.84 |
| | 18 | 15 | 0.86 | 5.0 | 22 | 0.86 |
| | 36 | 12 | 0.81 | 8.1 | 18 | 0.82 |
| | 60 | 8.4 | 0.77 | 9.3 | 14 | 0.78 |
| | 72 | 8.9 | 0.77 | 11 | 15 | 0.80 |
| | 96 | 9.9 | 0.78 | 15 | 12 | 0.78 |
| S30400 | 6 | 8.0 | 0.87 | 7.4 | 13 | 0.87 |
| | 18 | 11 | 0.88 | 12 | 14 | 0.89 |
| | 36 | 8.7 | 0.87 | 18 | 13 | 0.89 |
| | 60 | 6.9 | 0.84 | 17 | 12 | 0.87 |
| | 72 | 6.4 | 0.84 | 15 | 13 | 0.87 |
| | 96 | 6.3 | 0.84 | 16 | 14 | 0.88 |
| S31603 | 6 | 19 | 0.86 | 16 | 11 | 0.86 |
| | 18 | 18 | 0.87 | 13 | 12 | 0.87 |
| | 36 | 9.4 | 0.84 | 6.9 | 14 | 0.84 |
| | 60 | 9.5 | 0.80 | 12 | 11 | 0.81 |
| | 72 | 10 | 0.81 | 9.6 | 12 | 0.80 |
| | 96 | 8.8 | 0.79 | 11 | 11 | 0.79 |
| S31635 | 6 | 22 | 0.87 | 5.6 | 16 | 0.86 |
| | 18 | 12 | 0.86 | 2.6 | 25 | 0.86 |
| | 36 | 19 | 0.70 | 2.1 | 43 | 0.74 |
| | 60 | 14 | 0.79 | 6.8 | 12 | 0.78 |
| | 72 | 10 | 0.79 | 3.9 | 18 | 0.79 |
| | 96 | 15 | 0.79 | 13 | 12 | 0.78 |
| S32205 | 6 | 39 | 0.83 | 1.8 | 60 | 0.83 |
| | 18 | 45 | 0.84 | 3.4 | 58 | 0.85 |
| | 36 | 34 | 0.83 | 4.1 | 50 | 0.83 |
| | 60 | 37 | 0.83 | 3.0 | 62 | 0.83 |
| | 72 | 29 | 0.77 | 2.7 | 49 | 0.79 |
| | 96 | 31 | 0.80 | 4.7 | 45 | 0.81 |

chlorides show lower $R_{pl}$ values than non carbonated samples with chlorides. The exposure conditions seem to be more determining for $R_{pl}$ than the compositions of stainless steels.

The mortar samples were submitted to anodic polarization tests to obtain more information about their relative corrosion resis tance. Some examples of the obtained results, plotted as Evans

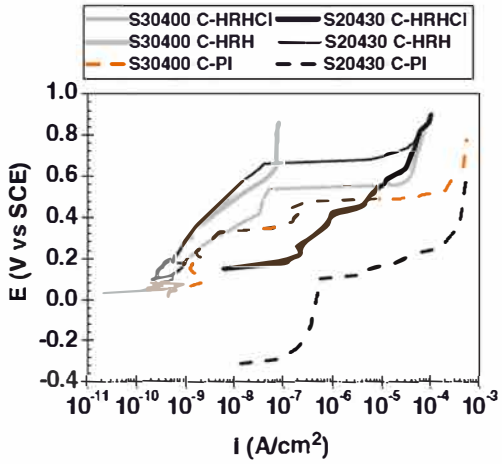


Fig. 11. Examples of the results obtained from the polarization tests in carbonated mortars.

diagrams, are shown in Fig. 11. The influence of the media and the stainless steel composition are reflected in the current density values where the potential increases. Samples are anodically polarized up to 900 mV vs. SCE. As water decomposition in carbonated mortars takes place at higher than 900 mV vs. SCE, no meaningful current increases take place in systems whose behavior is very good (curve of S30400 in C HRH in Fig. 11). So, all detected current increases found in Fig. 11 (but the previously indicated) correspond to the development of a corrosive attack.

It must be pointed out that in the anodic polarization of the S20430 in C HRHCl no passive region appears in the curve (Fig. 11), though the system exhibits a $E_{corr}$ characteristic of the passive state (Fig. 4), and the $R_t$ values measured without polarization confirm the passivity (Fig. 10). Thus, the corrosion rate of the stainless steel at $E_{corr}$ is negligible, but a small anodic polarization is able to break the passive state. Moreover, it is important to point out that the S20430 grade, under C Pl, can easily reach very dangerous corrosion rates under moderate anodic polarizations. Thus, the use of this grade can be risky in extremely aggressive environments.

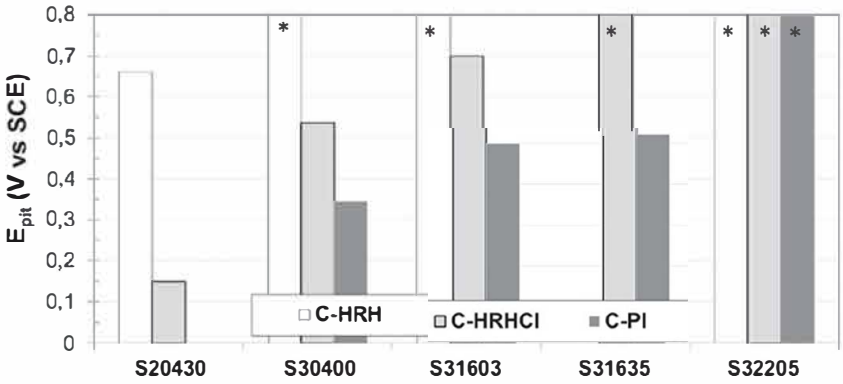


Fig. 12. $E_{pit}$ values obtained from the anodic polarization of the reinforced mortar samples after the 8-year exposure. Data marked with * correspond to systems where the polarization does not cause pitting corrosion.

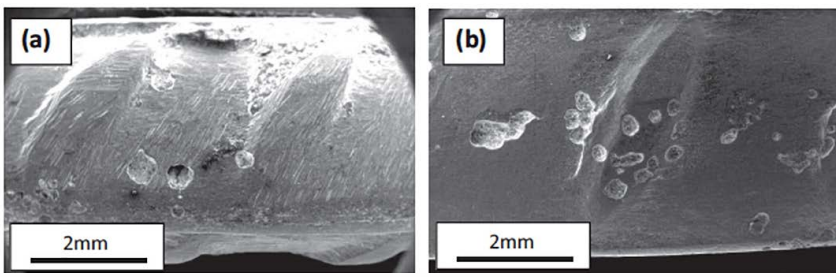


Fig. 13. SEM images of the morphology of the attack on S20430 corrugated bars: (a) in C-HRH; (b) in C-HRHCl.

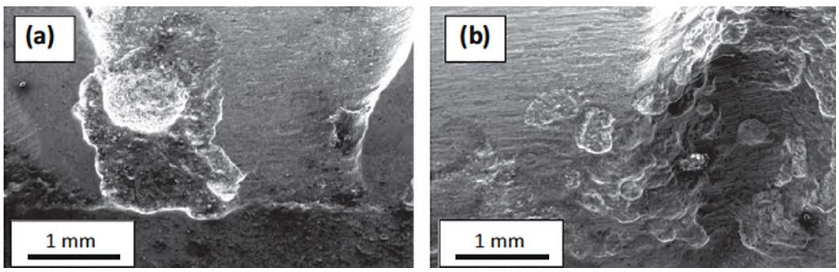


Fig. 14. SEM images of the morphology of the attack on traditional austenitic grades embedded in carbonated mortar: (a) S30400 in C-HRHCl; (b) S31635 in C-Pl.

The pitting potential ($E_{pit}$) obtained from polarization curves as those in the examples in Fig. 11 are plotted in Fig. 12 for the dif ferent studied systems. The $E_{pit}$ values correspond to potentials where the anodic current densities show a sharp increase and they are usually defined for current ranges between $2 \cdot 10^{-8}$ and $5 \cdot 10^{-8}$ A/cm$^2$. Value for S20430 in C PI is not included as this system spontaneously became active during the exposure. Value corresponding to S31665 in C HRH is not included because at the end of the experiments, when the morphology of the attack was analyzed, it was seen that corrosion was caused under the isolating tape that covers the bar in the mortar air interface. As the polarization caused corrosion in a crevice created by the experimental set up, those results were not taken into account for the study.

The duplex S32205 does not corrode under polarizations in any of the conditions, confirming the exceptional results of this mate rial as reinforcement seen with non carbonated mortar samples [11]. For the austenitic stainless steels, the C PI confirms to be the most aggressive condition of the 3 considered in this article.

Tested stainless steels seem to be able to guarantee the durabil ity of carbonated structures when no chlorides are present. Only S20430 pits under polarization in C HRH, but at quite high anodic overpotentials.

After the anodic polarization, the caused attack was allowed to evolve for 1 additional year under the exposure conditions. Then, the mortar samples were broken and the location and morphology of the attack on the stainless steel bars were studied. In Fig. 13, examples of the attack developed on S20430 can be seen. S20430 in absence of chlorides and when the corrosion is provoked by ano dic polarization in carbonated mortars corrodes in a localized way (Fig. 13(a)). Round pits are observed on the surface of the material, but pits with less geometrical shape appear on the regions of the surface with a most strained microstructure. The relationship between high strained microstructures of austenitic stainless steel corrugated bars and their corrosion behavior has already been ana lyzed in depth in previous papers based on results from solution tests [22]. A similar morphology of the attack is observed on the surface of S20430 after C PI and C HRHCl conditions (Fig. 13(b)). The main influence of the presence of chlorides in the medium is an increase in the intensity of the damage.

In Fig. 14, examples of the morphology of the attack observed in other more alloyed stainless steels are shown. As it has been reported for non carbonated media [11], S30400 (Fig. 14(a)) tends to develop big pits always located on the corrugations and in the most strained region of the bar. This behavior has been related with the high deformation level of this corrugated material [11].

In austenitic grades with Mo (Fig. 14(b)), localized attack with a low penetrating shape has been observed. This is the same mor phology of attack observed for these grades in non carbonated mortars [11]. However, in carbonated mortars, a certain relation ship between the localization of the attack and the most strained region of the surface has been detected. This relationship has not been previously observed for these materials in non carbonated mortars [11].

## 4. Conclusions

1. Low Ni, austenitic S20430 corrugated bars are especially prone to suffer a low intensity corrosive attack in carbonated mortars with chlorides. Moreover, the corrosion rate can easily increase under moderate anodic polarizations.
2. Corrosion on S20430 reinforcements progress faster in carbon ated mortars than in non carbonated ones when they are par tially immersed in 3.5% NaCl despite of the lower amount of diffused chlorides into the former.
3. Duplex S32205 is immune to corrosion in the carbonated mor tar with chlorides, even in partial immersion conditions and under high anodic polarizations.
4. Austenitic stainless steel reinforcements could suffer localized corrosion in carbonated mortar with chlorides when they are submitted to high anodic polarizations.

## Acknowledgment

The present work was funded by the Spanish Ministry of Science and Innovation through the Project reference BIA2007 66491 C02.

## References

[1] S. Talukdar, N. Banthia, Carbonation in concrete infrastructure in the context of global climate change: development of a service lifespan model, Constr. Build. Mater. 40 (2013) 775–782.
[2] P. Dangla, W. Dridi, Rebar corrosion in carbonated concrete exposed to variable humidity conditions. Interpretation of Tuutti's curve, Corros. Sci. 51 (2009) 1747–1756.
[3] Q. Huang, Z. Jiang, W. Zhang, X. Gu, X. Dou, Numerical analysis of the effect of coarse aggregate distribution on concrete carbonation, Constr. Build. Mater. 37 (2012) 27–35.
[4] S.-H. Han, W.-S. Park, E.-I. Yang, Evaluation of concrete durability due to carbonation in harbor concrete structures, Constr. Build. Mater. 48 (2013) 1045–1049.
[5] P.F. Marques, C. Chastre, A. Nunes, Carbonation service life modelling of RC structures for concrete with Portland and blended cements, Cem. Concr. Comput. 37 (2013) 171–184.
[6] E. Zornoza, P. Garcés, J. Mozó, M.V. Borrachero, J. Payá, Accelerated carbonation pf cement pastes partially substituted with fluid catalytic cracking catalyst residue (FC3R), Cem .Concr. Comput. 31 (2009) 134–138.
[7] F. Pacheco Torgal, S. Miraldo, J.A. Labrincha, J. De Brito, An overview on concrete carbonation in the context of eco-efficient construction: evaluation use of SCMs and/or RAC, Constr. Build. Mater. 36 (2012) 141–150.
[8] S. Talukdar, N. Banthia, J. Grace, S. Cohen, Carbonation in concrete infrastructure in the context of global climate change: Part II – Canadian urban simulations, Cem. Concr. Comput. 34 (2012) 931–935.
[9] D.V. Val, M.G. Stewart, Life-cycle cost analysis of reinforced concrete structures in marine environments, Struct. Saf. 25 (2003) 343–362.
[10] E. Medina, J.M. Medina, A. Cobo, D.M. Bastidas, Evaluation of mechanical and structural behaviour of austenitic and duplex stainless steel reinforcements, Constr. Build. Mater. 78 (2015) 1–7.
[11] A. Bautista, E.C. Paredes, F. Velasco, S.M. Alvarez, Corrugated stainless steels embedded in mortar for 9 years: corrosion results of non-carbonated, chloride-contaminated samples, Constr. Build. Mater. 93 (2015) 350–359.
[12] L. Freire, M.J. Carmezim, M.G.S. Ferreira, M.F. Montemor, The passive behaviour of AISI 316 in alkaline media and the effect of pH: a combined electrochemical and analytical study, Electrochim. Acta 55 (2012) 6174–6181.
[13] A. Bautista, G. Blanco, F. Velasco, A. Gutiérrez, L. Soriano, F.J. Palomares, et al., Changes in the passive layer of corrugated, low Ni, austenitic stainless steel due to the exposure to simulated pore solutions, Corros. Sci. 51 (2009) 785–792.
[14] A. Bautista, G. Blanco, F. Velasco, Corrosion behaviour of low-nickel austenitic stainless steels reinforcements: a comparative study in simulated pore solutions, Cem. Concr. Res. 36 (2006) 1922–1930.
[15] M. Moreno, W. Morris, M.G. Alvarez, G.S. Duffó, Corrosion of reinforcing steel in simulated concrete pore solutions: effect of carbonation and chloride content, Corros. Sci. 46 (2004) 2681–2699.
[16] U. Angst, B. Elsener, C.K. Larsen, O. Vennesland, Critical chloride content in reinforced concrete – a review, Cem. Concr. Res. 39 (2009) 1122–1138.
[17] V.K. Gouda, Corrosion inhibition of reinforcing steel. I. Immersed in alkaline solutions, Br. Corros. J. 5 (1970) 204–208.
[18] L. Li, A.A. Sagüés, Chloride concentration threshold of reinforcing steel in alkaline solutions – open-circuit immersion tests, Corrosion 57 (2001) 19–28.
[19] A. Ipavec, T. Vuk, R. Gabrosek, V. Kaucic, Chloride binding into hydrated blended cements: the influence of limestone and alkalinity, Cem. Concr. Res. 48 (2013) 74–85.
[20] F.P. Glasser, J. Marchand, E. Samson, Durability of concrete – degradation phenomena involving detrimental chemical reactions, Cem. Concr. Res. 38 (2008) 226–246.
[21] X. Shi, N. Xie, K. Fortune, J. Gong, Durability of steel reinforced concrete in chloride environments: AN overview, Constr. Build. Mater. 30 (2012) 125–138.
[22] E.C. Paredes, A. Bautista, S.M. Alvarez, F. Velasco, Influence of the forming process of corrugated stainless steels on their corrosion behaviour in simulated pore solutions, Corros. Sci. 58 (2012) 52–61.
[23] R.D. Moser, P.M. Singh, L.F. Kahn, K.E. Kurtis, Chloride-induced corrosion resistance of high-strength stainless steels in simulated alkaline and carbonated concrete pore solutions, Corros. Sci. 57 (2012) 241–253.

[24] S. Fajardo, D.M. Bastidas, M.P. Ryan, M. Criado, D.S. McPhail, R.J.H. Morris, et al., Low energy SIMS characterization on passive oxide films formed on a low-nickel stainless steel in alkaline media, Appl. Surf. Sci. 288 (2014) 423–429.
[25] C. Monticelli, M. Criado, S. Fajardo, J.M. Bastidas, M. Abbottoni, A. Balbo, Corrosion behaviour of a low Ni austenitic stainless steel in carbonated chloride-polluted alkali-activated fly ash mortar, Cem. Concr. Res. 55 (2014) 49–58.
[26] RILEM, Draft recommendation for repair strategies for concrete structures damaged by reinforcement corrosion, Mater. Struct. 27 (1994) 415–438.
[27] P. Castro, A.A. Sagües, E.I. Moreno, L. Maldona, J. Genescá, Characterization of activated titanium solid reference electrodes for corrosion testing of steel in concrete, Corrosion 52 (1996) 609–617.
[28] K. Kinoshita, M.J. Madou, Electrochemical measurements on Pt, Ir, and Ti oxides as pH probes, J. Electrochem. Soc. 131 (1984) 1089–1094.
[29] R.K. Dhir, M.R. Jones, H.E.H. Ahmed, Determination of total and soluble chlorides in concrete, Cem. Concr. Res. 20 (1990) 579–590.
[30] A. Bautista, G. Blanco, F. Velasco, A. Gutiérrez, S. Palacín, L. Soriano, et al., Passivation of duplex stainless steels in solutions simulating chloride-contaminated concrete, Mater. Constr. 57 (2007) 17–32.
[31] E. Zornoza, J. Payá, P. Garcés, Chloride-induced corrosion of steel embedded in mortars containing fly ash and spent cracking catalyst, Corros. Sci. 50 (2008) 1567–1575.
[32] C.K. Glass, N.R. Buenfeld, The presentation of the chloride threshold level for corrosion of steel in concrete, Corros. Sci. 39 (1997) 1001–1013.
[33] C. Arya, N.R. Buenfeld, J.B. Newman, Factor influencing the chloride binding in concrete, Cem. Concr. Res. 20 (1990) 291–300.
[34] H.-W. Song, S.-J. Kwon, Permeability characteristics of carbonated concrete considering capillary pore structure, Cem. Concr. Res. 37 (2007) 909–915.
[35] L. Freire, M.J. Carmezim, M.G.S. Ferreira, M.F. Montemor, The electrochemical behaviour of stainless steel AISI 304 in alkaline solutions with different pH in the presence of chlorides, Electrochim. Acta 56 (2011) 5280–5289.
[36] H. Luo, C.F. Dong, X.G. Li, K. Xiao, The electrochemical behavior of 2205 duplex stainless steel in alkaline solutions with different pH in the presence of chlorides, Electrochim. Acta 64 (2012) 211–220.
[37] M. Serdar, L.V. Sulj, D. Bjegovic, Long-term corrosion behaviour of stainless reinforcing steel in mortar exposed to chloride environment, Corros. Sci. 69 (2013) 149–157.
[38] C.M. Abreu, M.J. Cristóbal, R. Losada, X.R. Novoa, G. Pena, M.C. Pérez, Long-term behaviour of AISI 304L passive layer in chloride containing medium, Electrochim. Acta 51 (2006) 1881–1890.
[39] P. Gu, S. Elliott, J.J. Beaudoin, B. Arsenault, Corrosion resistance of stainless steel in chloride contaminated concrete, Cem. Concr. Res. 26 (1996) 1151–1156.
[40] T. Ishida, K. Kawai, R. Sato, Experimental study on decomposition processes of Friedel's salt due to carbonation, in: K. Kovler (Ed.), Proc. Int. RILEM-JCI Seminar on Concrete Durability (ConcreteLife'06), Ein-Bokek (Israel), 2006, pp. 51–58.